

Design and Experiment on Zinc-air Battery Continuous Power Controller Based on Microcontroller

Yanjun Xiao*, Ran Jing, Haiping Song, Na Zhu, Huan Yang

School of Mechanical Engineering, Hebei University of Technology, Tianjin, 300130, China
 xyj_hebut@163.com

The Zinc-air batteries continuous power generation which is designed by our task group realizes the discharge of zinc electrode in motion and solves the problem of self-discharge of Zinc-air battery. Zinc-air battery continuous power generation control system is designed in this paper to realize the automatic operation of the Zinc-air batteries continuous power generation and improve the generation efficiency of Zinc-air batteries continuous power generation. The design of the device is based on the combination of mechanical power system and electrical control technology. This paper uses PIC16F877A microcontroller as the control core and the main electrical equipment of Zinc-air battery for continuous power generation devices (analog acquisition equipment and stepper motor) with electrical control technology is analysed. The design ideas in software is modular design. Software control flow chart for stepper motors and analog acquisition is drawn. This paper is tested on controller, Result of test shows that the controller is able to meet the control requirements of continuous power plant and verify the feasibility of the controller.

1. Introduction

Zinc air battery is a kind of semi fuel cell, which has the advantages of high specific energy, low cost and stable discharge voltage (Ning et al., 2012). The problems of the self-discharge of the zinc air battery in the process of using, caused some difficulties for the promotion of the market. Our task group design the Zinc-air batteries continuous power generation for solves the problem of self-discharge of Zinc-air battery. Zinc pole pieces is dragged by the coiling mechanism and the unwinding mechanism to make it slow motion in the electrolyte. Chemical reaction of Zinc pole pieces and oxygen under the action of electrolyte in the movement process of Zinc pole pieces. This chemical reaction caused the gains and losses of cathode electron and anode electron to produce electric current (Hernández-Fernández et al., 2010; Jencarova et al., 2012). This way realizes the zinc air battery to power generation in the movement. When no power is needed, the Zinc pole pieces is quickly withdrawn from the electrolyte and the electrochemical reaction is stopped. The Zinc-air batteries continuous power generation solves the problem of self-discharge of Zinc-air battery. Zinc-air batteries continuous power generation capable of exerting the advantages of Zinc-air batteries to better meet the needs of the market.

The Zinc-air batteries continuous power generation which is designed by our task group realizes the discharge of zinc electrode in motion and solves the problem of self-discharge of Zinc-air battery. Because of simple structure and powerful real-time of the embedded system, it demonstrated a distinct advantage in electrical control technology (Lozoya et al., 2013). So this paper choose PIC16F877A microcontroller as control core of embedded control system.

In this paper, the hardware and software of embedded controller of Zinc-air battery continuous power generation are researched and developed. We also build embedded control system platform for the related critical Control Technology, software and hardware are tested to verify the feasibility of the program. The research has important theoretical and practical effect on the development and application of the new energy in China and the world.

2. Design and analysis of the overall mechanical power system

The structure diagram of Zinc-air batteries continuous power generation is shown in Figure 1.

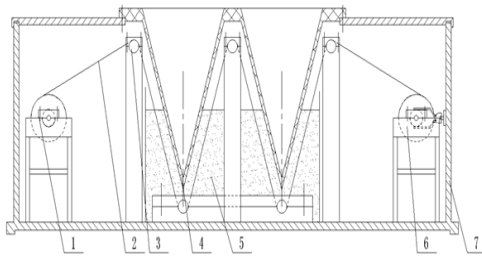


Figure 1: Structure diagram of Zinc-air batteries continuous power generation: 1. Unwinding agency 2. anode plate 3. Transmission 4. Cathode plate 5. Battery compartment 6. Anode output 7. winding mechanism

The power system of Zinc-air batteries continuous power generation is to achieve power from Zinc pole pieces in motion(Sun et al., 2014). during the electricity generation, unreacted zinc pole pieces are dragged by winding mechanism 7, Zinc pole piece enter the battery compartment 5 by unwinding institution 1 through the transport mechanism 3. The zinc electrode is combined with oxygen adsorbed by the cathode plate, and the chemical reaction about them is carried out in the KOH solution(VladimirM et al., 2014).Zinc pole piece comes into a smooth low speed motion to ensure adequate electrochemical reaction when the condition is satisfied Generation. Velocity is determined by the discharge voltage, discharge current and temperature of the electrolyte. Zinc pole piece is quickly withdraw from the electrolyte when power generation is needed, so that electrochemical reaction automatically stops because of lacking of anode material.

3. Overall design of Zinc-air battery continuous power controller

In this paper, according to the analysis of mechanical power system: Zinc pole pieces are mainly driven by the two stepper motor which is in the winding and unwinding mechanism. However, motor control mainly contained high-speed smooth movement of zinc pole pieces access to the electrolyte and Smooth motion at low speed after normal power. This condition is achieved by the controller control the stepper motor by using the PWM algorithm and the stepper motor drive circuit.In this power plant, the velocity is as a measure of the utilization of zinc pole piece. Therefore, this controller requires an analogy acquisition module collecting discharge voltage, discharge current, and temperature of the electrolyte in real-time, the velocity of zinc pole piece is obtained by the control algorithm. In order to maximize the utilization of the zinc pole piece, Zinc pole piece position and velocity feedback ccircuit are added to the controller to form a closed-loop system. Controller and MCGS communication through the serial communication circuit to achieve human-computer interaction. Power management module power supply for overall system.Switch button control the start and stop of the control system. The specific structure of the Zinc-air batteries continuous power generation control system is shown in Figure 2.

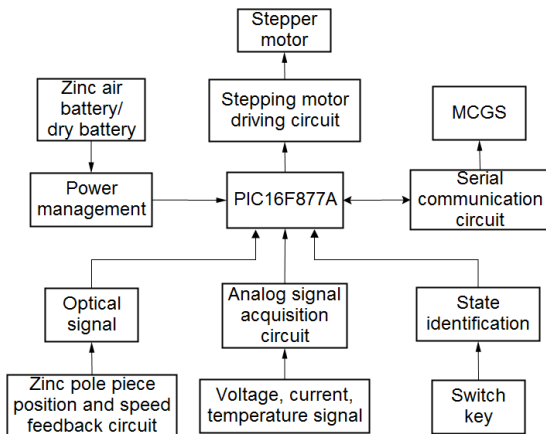


Figure 2: The diagram of Zinc-air batteries continuous power generation

4. The main hardware circuit design

In this paper, the design of the single circuit is based on the overall scheme. Commissioning and installation are considered to the system, it uses a modular design. Hardware circuit consists of five small modules, the Interactive interface is a 7-inch touch screen MCGS. There are minimum system, stepper motor driving circuit, serial communication circuit, Zinc pole piece position and speed feedback circuit, analog signal acquisition circuit and power management circuit. This article describes the following two hardware circuits.

4.1 Circuit Design of Analog Acquisition

The hardware circuit is using PIC16F877A microcontroller as the core of the analog data acquisition and analysis system, A / D conversion circuit whose core chip is AD7706 is also included (Yang and Lu, 2007). Figure 3 is a circuit diagram of a basic application AD7706 in this system. The analog acquisition circuit including voltage and current acquisition circuit and temperature acquisition circuit.

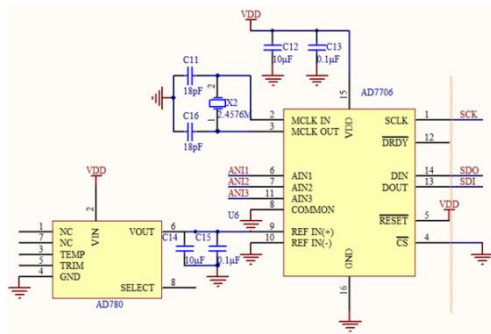


Figure 3: AD7706 Application Circuit

The discharge voltage of the Zinc-air batteries is between 0 and 1.4 V, the discharge voltage which can be directly sampled without magnification can be sent into analog input channel ANI1 of AD7706 chip after filtering. Current collection applies the method that converts it to required accuracy voltage which is sent to the ANI2 channel of the AD7706 chip by 1 mΩ precision resistors and operational amplifiers MCP601. Hardware circuit is shown in Figure 4.

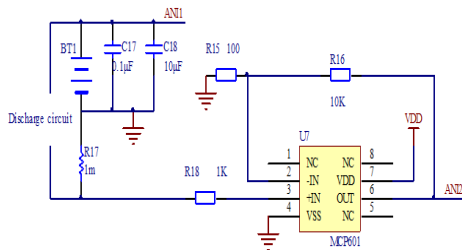


Figure 4: Voltage and current acquisition circuit

Temperature of zinc-air battery power plant range from -100 °C to 500 °C, the value of PT100 (Liu et al., 2010) resistor range from 90 Ω to 120 Ω, Good linear change and the rate of change is 0.385 Ω/°C. To eliminate the error caused by the measurement accuracy on the resistance of connect the wire, bridge circuit is used to maximized reduce the error. PT100 connection circuit is shown in Figure 3. PT100 minimum output is 90 Ω which satisfied Eq(1), bridge balance, the voltage difference between lines 1 and lines 2 is U12, 0 V, error can be eliminated.

$$U_{12} = \left(\frac{R8}{R8 + R9} - \frac{R_{pt} + 2r}{R_{pt} + 90 + 4r} \right) \times VDD \tag{1}$$

The value of VDD is 5 V, when the value of Rpt range from 90 Ω to 120 Ω, the value of U12 range from -0.4 V to 0 V by the Eq(1). The measured voltage is converted to the basic voltage which range from 0 V to 2.5 V by using the basic differential amplifier circuit, the got voltage meets the sampled accuracy of the analog input circuit. Shown as Figure 6. From Figure 5 we can get Eq(2).

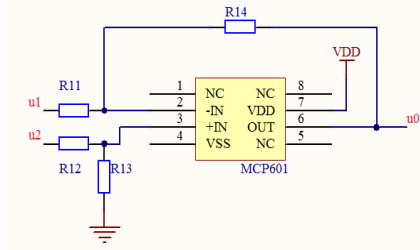


Figure 5: The basic differential amplifier circuit

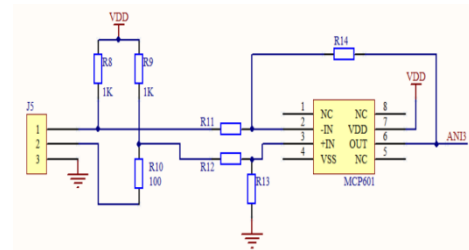


Figure 6: Temperature acquisition circuit

$$u_0 = \frac{R_{14}}{R_{11}}(u_2 - u_1) \tag{2}$$

In this system, (U2-U1) is 0 to 0.4 V, U0 is 2.5 V, therefore, the ratio of R14 and R14 should be 25/4. R14 and R13 are selected as 2.5 KΩ, then R11, R12 are 400 Ω. Figure 6 is a temperature sampling circuit.

4.2 Control Circuit Design of Stepper Motor

The Stepper motor is driven by pulse generator and drive. Pulse generator and stepper drive are collectively known as stepper motor driver module, control operation of the motor through access to the PWM pulse (Guan et al., 2014). The system uses a way that stepper motor driver chip L298 and stepper motor control chip L297 are combined to control the stepper motor (Wu and Lu, 2011). The Stepper motor is controlled by the PWM mode. Figure 7 is a stepper motor control circuit.

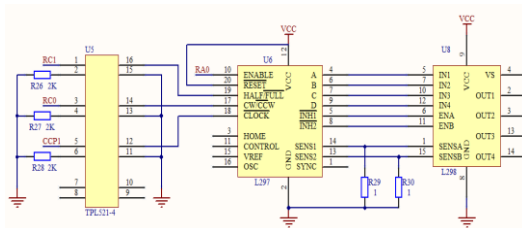


Figure 7: Stepper motor control circuit

5. Software design

The embedded system of Zinc-air battery continuous power controller which used the modular design concept has main program module, stepping motor control module, high-speed input module and analog acquisition module. The main program module not only coordinates all modules, but also communicates with the touchscreen.

The analog acquisition module consists of three Sub-module: SPI Configuration, AD7706 drive and interruption. In the mode of SPI, PIC16F877A is the controller and AD7706 is the follower. The process of the analog acquisition module is shown in figure 8.

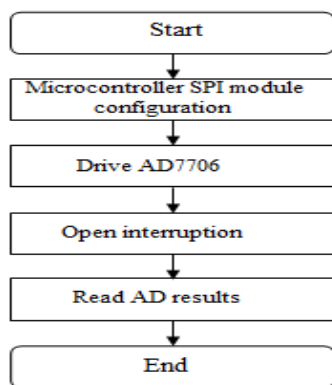


Figure 8: Analog acquisition module processes

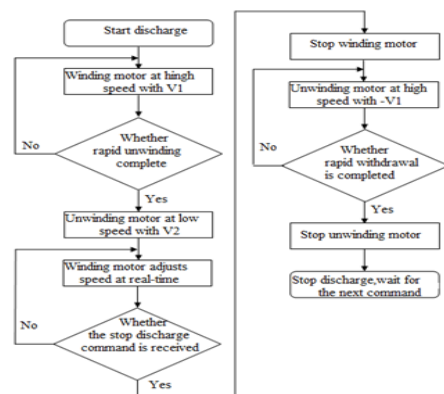


Figure 9: Stepper motor sports flowchart

Zinc-air battery continuous power controller contains two stepping motors: winding motor and unwinding motor. The motion process of stepping motors is shown in Figure 9, the set values of V1 and V2 is relate to the zinc pole piece’s width, thickness and motor parameters. -V1 represents unwinding motor runs at the rate of V1 and in the opposite direction.

6. Online test baesd on MCGS with PIC16F877A microcontroller

Upon completion of the controller embedded hardware and software development, hardware and software are in actual commissioning to prove the availability and reliability of embedded systems. The system follows the principle that after the hardware testing is software testing during debugging, hardware and software debug of each function after the exclusion of the hardware error.

6.1 Hardware and Software Test of Stepper Motor

The core of stepper motor control module is reversing control and high and low speed switching, involve switch data sending and integer data transmission and reception. Figure 10 shows the corresponding relationship between switch data objects with the channels. The function that Motor start and stop and reversing switch commands are achieved by controlling corresponding pin of Microcontroller high and low output, Frequency plus and minus is calling subroutine of object to achieve Increasing or decreasing the motor speed.

Aisle	Corresponding data objects	Channel type	Cycle
3	Analytic channel	Analytic channel	1
4	Motor start and stop	M00	1
5	Motor switching	M01	1
6	Reversing switch	M02	1
7	Frequency plus	M03	1
8	Frequency reduce	M04	1
9	Automatic operation	M05	1
10	Automatic stop	M06	1
11		M07	1
12		M08	1
13		M09	1

Figure 10: Correspondence between the switch data objects with the channels

Motor frequency input box which consist with the motor frequency of the microcontroller correspond with integer channel I0. After input 20 Hz on the touch screen shown in Figure 11, click motor start button, then Stepper motor is at low speed, Stepper motor output frequency chart is shown as figure 12, pulse frequency which consists with the input details 19.99 Hz from figure 13.

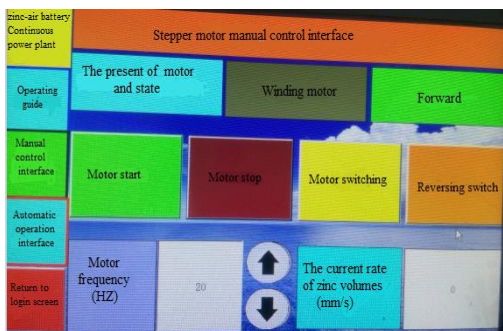


Figure 11: Manual control interface of winding stepper motor at low start



Figure 12: Frequency output map of motor at low speed rotational

Click motor stop button, motor switch button, motor reversing switch button, and enter 2000 Hz in the input box, as is shown in figure 13, then the motor reverse rotates at high speed, motor rotation frequency output is shown in figure 14, pulse frequency consistent with the input data is 1.991 KHz.

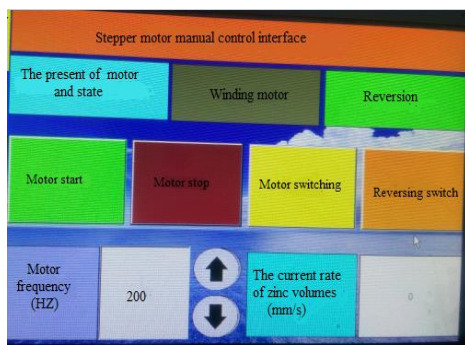


Figure 13: Manual control interface of unwinding motor at high start

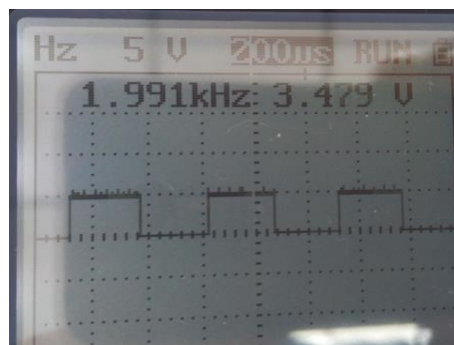


Figure 14: Frequency output map of stepper motor at high speed rotational

7. Conclusions

Based on the characteristic of combination of mechanical power system and electrical control, the paper analyzed the Zinc-air battery for continuous power generation devices. This article developed the hardware and software of embedded system. The paper tests the control system with the existing conditions, and ensures the accuracy and stability of the software and hardware of each module and to create the theoretical significance and practical value for the development and application of new energy.

Acknowledgments

This work was financially supported by the Hebei Province Natural Science Fund Project 'The research on the theory and method of the integration design about the control system of continuous power and power management of the zinc-air battery based on active balance', whose number is E2013202230.

Reference

- Guan X.C., Shen B.Y., 2014, Application research of stepper motor control with TMS320F2812, Applied Mechanics and Materials, 556(562), 2544-2548, DOI: 10.4028/www.scientific.net/AMM.556-562.2544
- Hernández F., Francisco J., De L.R., Antonia P., Ginestá A., Sánchez S., Lozano L.J., Moreno J., Godínez C., 2010, Use of ionic liquids as green solvents for extraction of Zn²⁺, Cd²⁺, Fe³⁺ and Cu²⁺ from aqueous solutions, Chemical Engineering Transactions, 21, 630-636, DOI: 10.3303/CET1021106
- Jencarova J., Luptakova A., 2012, The elimination of heavy metal ions from waters by biogenic iron sulphides, Chemical Engineering Transactions, 28, 205-210, DOI: 10.3303/CET1228035
- Liu J.G., Li Y.K., Zhao H.Y., 2010, temperature measurement system based on PT100, Proceedings - International Conference on Electrical and Control Engineering, 296-298, DOI: 10.1109/iCECE.2010.79
- Lozoya C., Velasco M., Martí P., 2008, The one-shot task model for robust real-time embedded control systems, IEEE Transactions on Industrial Informatics, 4, 164-174, DOI: 10.1109/TII.2008.2002702
- Ning X.H., Phadke S., Chung B., Yin H.Y., Burke P., Sadoway D.R., 2014, Self-healing Li-Bi liquid metal battery for grid-scale energy storage, Journal of Power Sources, 275, 370-376, DOI: 10.1016/j.jpowsour.2014.10.173
- Sun Y.G., Qiang H.Y., Yang K.R., Chen Q.L., Dai G.W., Dong M., 2014, Experimental design and development of heave compensation system for marine crane, Mathematical modelling of engineering problems, 1, 15-20
- Volgin V.M., Kabanova T.B., Davydov A.D., 2014, Modeling of metal electrodeposition through colloidal crystal mask, Chemical Engineering Transactions, 41, 331-336, DOI: 10.3303/CET1441056
- Wu H.C., Lu F., 2011, Development of embedded control system of micro-flow variable plunger pump based on frequency control, Advanced Materials Research, 317(319), 1568-1572, DOI: 10.4028/www.scientific.net/ARM.317-319.1568
- Yang S.H., Lu H.S., 2007, Experimental study on photoelectric data acquisition system with high precision, optical technique, 5, 791-795, DOI: 10.13741/j.cnki.11-1879/o4.2007.05.043